

Access to Stable Metalloradical Cations with Unsupported and Isomeric Metal–Metal Hemi-Bonds**

Xin Zheng, Xingyong Wang, Zaichao Zhang, Yunxia Sui, Xinping Wang,* and Philip P. Power*

Abstract: Metalloradical species $[\text{Co}_2\text{Fv}(\text{CO})_4]^{+\bullet}$ ($\mathbf{1}^{+\bullet}$, Fv = fulvalenediyl) and $[\text{Co}_2\text{Cp}_2(\text{CO})_4]^{+\bullet}$ ($\mathbf{2}^{+\bullet}$, Cp = $\eta^5\text{-C}_5\text{H}_5$), formed by one-electron oxidations of piano-stool cobalt carbonyl complexes, can be stabilized with weakly coordinating polyfluoroaluminate anions in the solid state. They feature a supported and an unsupported (i.e. unbridged) cobalt–cobalt three-electron σ bond, respectively, each with a formal bond order of 0.5 (hemi-bond). When Cp is replaced by bulkier Cp* (Cp* = $\eta^5\text{-C}_5\text{Me}_5$), an interchange between an unsupported radical $[\text{Co}_2\text{Cp}^*_2(\text{CO})_4]^{+\bullet}$ (anti- $\mathbf{3}^{+\bullet}$) and a supported radical $[\text{Co}_2\text{Cp}^*_2(\mu\text{-CO})_2(\text{CO})_2]^{+\bullet}$ (trans- $\mathbf{3}^{+\bullet}$) is observed in solution, which cocrystallize and exist in the crystal phase. $\mathbf{2}^{+\bullet}$ and anti- $\mathbf{3}^{+\bullet}$ are the first stable thus isolable examples that feature an unsupported metal–metal hemi-bond, and the coexistence of anti- $\mathbf{3}^{+\bullet}$ and trans- $\mathbf{3}^{+\bullet}$ in one crystal is unprecedented in the field of dinuclear metalloradical chemistry. The work suggests that more stable metalloradicals of metal–metal hemi-bonds may be accessible by using metal carbonyls together with large and weakly coordinating polyfluoroaluminate anions.

It is of fundamental importance to understand the nature of metal–metal bonds.^[1] Compared with those supported by bridging ligands, unsupported metal–metal bonds are simpler and have attracted particular interest.^[2] Understanding of the metal–metal interactions in the paramagnetic metal complexes is especially crucial for the fields of metalloproteins^[3] and metal-containing functional materials.^[4] A number of supported dinuclear metalloradicals with two metal atoms

held together to form a bond by a bridging ligand are known.^[5] In contrast, stable but unsupported dinuclear metalloradicals are rare. Recently two unsupported dinuclear metalloradicals were isolated and studied by single crystal X-ray diffraction, that is, $[\text{M}_2\text{Cp}_2(\text{CO})_4(\text{PMe}_3)_2]^{+\bullet}$ (M = Mo and W), where two metal atoms are held together by a multiple bond (bond order = 1.5) with assistance from the electron-donating ligand PMe_3 .^[6]

Cobalt complexes have been widely used as efficient catalysts for organic transformations and C–F bond activations,^[7] but the chemistry of dicobalt metalloradicals is relatively underdeveloped. Very recently, a radical cation with a cobalt–cobalt bond supported by cyclic alkyl amino carbene ligands was reported.^[8] Electrochemical experiments have shown that piano-stool cobalt carbonyl complexes $\text{Co}_2\text{Fv}(\text{CO})_4$ and $\text{RCo}(\text{CO})_2$ (R = Cp or Cp*) could undergo one-electron oxidation to form dimer radical cations in solution,^[9] but the radical salts were not isolable due to instability and their crystal structures remain unknown. Recently we have succeeded in stabilization and isolation of radical cations $\text{NapE}_2\text{Ph}_2^{+\bullet}$ (E = S, Se; Nap = naphthalene) that feature a S–S or Se–Se three-electron σ bond,^[10] which prompted us to investigate the oxidation of transition metal complexes. In this paper we report the isolation and crystal structures of cobalt carbonyl radical cations $[\text{Co}_2\text{Fv}(\text{CO})_4]^{+\bullet}$ ($\mathbf{1}^{+\bullet}$), $[\text{Co}_2\text{Cp}_2(\text{CO})_4]^{+\bullet}$ ($\mathbf{2}^{+\bullet}$) and $[\text{Co}_2\text{Cp}^*_2(\text{CO})_4]^{+\bullet}$ ($\mathbf{3}^{+\bullet}$), which feature supported, unsupported and isomeric cobalt–cobalt hemi-bonds, providing the first stable thus isolable examples of unsupported metal–metal hemi-bonds.

$\text{Co}_2\text{Fv}(\text{CO})_4$ was treated with one equiv of $\text{Ag}[\text{Al}(\text{OR}_{\text{Me}})_4]$ ($\text{OR}_{\text{Me}} = \text{OC}(\text{CF}_3)_2\text{Me}$)^[11] in CH_2Cl_2 at 0 °C to afford a reddish brown solution of the radical cation $\mathbf{1}^{+\bullet}$ (Scheme 1). A green solution of radical cation $\mathbf{2}^{+\bullet}$ was obtained by the reaction of $\text{CpCo}(\text{CO})_2$ with a half equiv of $\text{Ag}[\text{Al}(\text{OR}_{\text{H}})_4]$ ($\text{OR}_{\text{H}} = \text{OC}(\text{CF}_3)_2\text{H}$)^[11] under similar conditions. Both colored solutions gradually faded and became intractable upon warming to room temperature or under reduced pressure. Crystals of $\mathbf{1}^{+\bullet}[\text{Al}(\text{OR}_{\text{Me}})_4]^-$ and $\mathbf{2}^{+\bullet}[\text{Al}(\text{OR}_{\text{H}})_4]^-$ were obtained by cooling reaction solutions in CH_2Cl_2 at –25 °C. The isolated salts are thermally stable under nitrogen atmosphere at room temperature and were studied by single-crystal X-ray diffraction, EPR, IR, and UV/Vis absorption spectroscopy, in conjunction with DFT calculations.

The crystal structures^[12] of cations $\mathbf{1}^{+\bullet}$ and $\mathbf{2}^{+\bullet}$ are shown in Figure 1 with structural parameters, some of which along with those of parent molecules $\text{Co}_2\text{Fv}(\text{CO})_4$ and $\text{CpCo}(\text{CO})_2$ are given in Table S2 in the Supporting Information. Contrary to the *transoid* configuration of neutral $\text{Co}_2\text{Fv}(\text{CO})_4$, cation $\mathbf{1}^{+\bullet}$ has a *cisoid* structure with a slightly bent fulvalenediyl

[*] X. Zheng,^[†] Dr. X. Wang,^[†] Y. Sui, Prof. X. Wang
State Key Laboratory of Coordination Chemistry
School of Chemistry and Chemical Engineering
Collaborative Innovation Center of Advanced Microstructures
Nanjing University, Nanjing 210093 (China)
E-mail: xpwang@nju.edu.cn

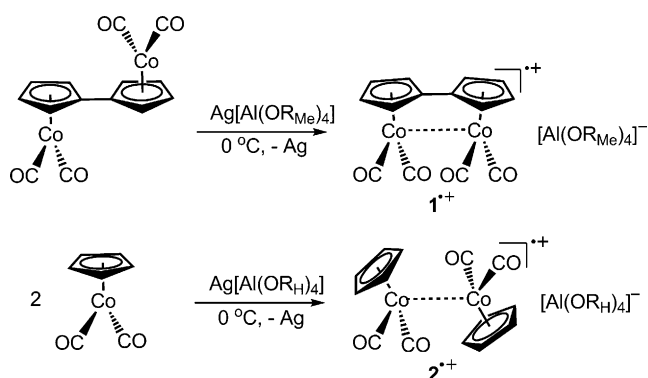
Dr. Z. Zhang
School of Chemistry and Chemical Engineering
Huaiyin Normal University, Huai'an 223300 (China)

Prof. P. P. Power
Department of Chemistry, University of California
Davis, CA 95616 (USA)
E-mail: pppower@ucdavis.edu

[†] These authors contributed equally to this work.

[**] We thank the National Natural Science Foundation of China (grant number 21171087, X.W.), the Major State Basic Research Development Program (grant number 2013CB922101, X.W.), the Natural Science Foundation of Jiangsu Province (grant number BK20140014, X.W.) and US National Science Foundation (grant number CHE-1263760, P.P.P.) for financial support.

Supporting information for this article is available on the WWW under <http://dx.doi.org/10.1002/anie.201503392>.



Scheme 1. Synthesis of supported (1^+) and unsupported (2^+) cobalt radical cations.

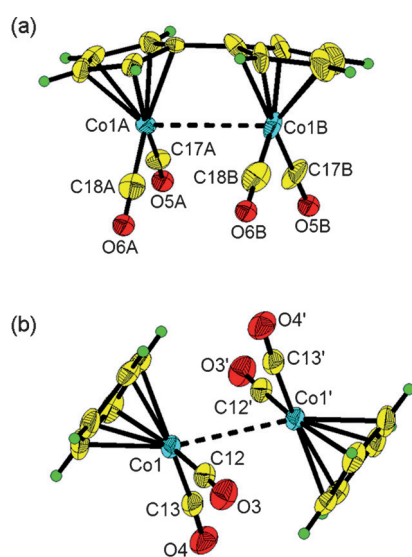


Figure 1. Thermal ellipsoid (50%) drawings of 1^+ and 2^+ . Yellow, carbon; green, hydrogen; red, oxygen; blue, Cobalt. a) 1^+ . Selected bond lengths [Å] and angles [deg]: Co1A–Co1B 3.0774(12), Co1A–C17A 1.771(5), Co1A–C18A 1.768(4), C17A–O5A 1.133(6), C18A–O6A 1.137(5), Co1B–C17B 1.778(5), Co1B–C18B 1.778(5), C17B–O5B 1.134(6), C18B–O6B 1.130(6); C17A–Co1A–C18A 95.1(2), C17B–Co1B–C18B 96.6(2), Co1A–C17A–O5A 178.8(4), Co1A–C18A–O6A 178.7(4), Co1B–C17B–O5B 178.0(5), Co1B–C18B–O6B 178.7(4); and b) 2^+ . Selected bond lengths [Å] and angles [deg]: Co1–Co1' 2.9593(10), Co1–C12 1.776(4), Co1–C13 1.795(4), C12–O3 1.135(4), C13–O4 1.124(4); C12–Co1–C13 97.90(16), Co1–C12–O3 177.2(3), Co1–C13–O4 177.4(3).

framework (Figure 1 a). Cation 2^+ has the *anti* conformation with a Co–Co bond that is not supported by any bridging ligand (Figure 1 b). In both cations, Co–C(O) bonds slightly lengthen while C–O bonds shorten and the OC–Co–CO angles are widened in comparison to the neutral parent molecules. The Co–Co bond lengths in 1^+ (3.0774(12) Å) and 2^+ (2.9593(10) Å) are longer than a Co–Co single bond length (2.5 Å)^[13] but shorter than the sum (3.84 Å) of the van der Waals radii of cobalt.

The previously calculated Co–Co bond lengths in 2^+ (3.137 Å) upon the consideration of solvent effect^{9a} differs

somewhat from that of the X-ray structure of 2^+ (Co–Co 2.959 Å). However, X-ray crystal structures of 2^+ and 1^+ were well reproduced by our DFT calculations without solvation (Table S2) at the level of B97-D/SVP/LanL2DZ including a long-range dispersion correction.^[14] Of particular note, the calculated Co–Co bond lengths in 2^+ (2.961 Å) and 1^+ (3.145 Å) compare closely those in the crystal structures. Also consistent with the experimental data, one-electron oxidation causes decrease of the C–O bond lengths, increase of the Co–C(O) bond lengths and widening of OC–Co–CO angles. The spin density distribution of 1^+ and 2^+ shows the unpaired electron is largely localized on Co atoms (1^+ 0.370×2 , 2^+ 0.436×2) with small amount on cyclopentadienyl ligands. The molecular orbitals of 1^+ and 2^+ display Co–Co σ^* antibonding SOMOs and Co–Co σ -bonding orbitals (Figure 2). The calculated Wiberg bond orders of Co–Co

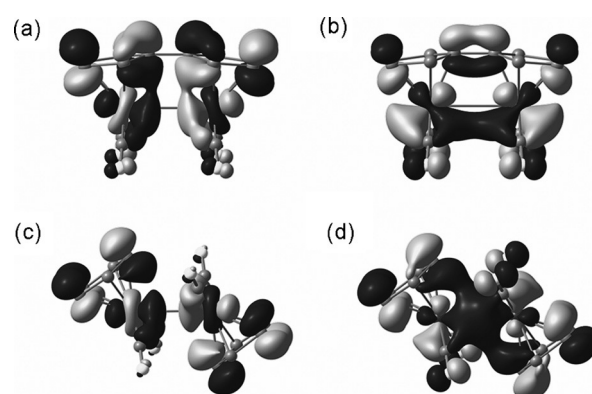


Figure 2. Frontier orbitals of 1^+ (top) and 2^+ (bottom). a,c) Co–Co σ^* -antibonding orbitals (SOMO). b,d) Co–Co σ -bonding orbitals (SOMO-1).

bonds in 1^+ (0.290) and 2^+ (0.392) are in accordance with the antibonding character of the SOMOs, supporting the hemi-bond formation. To check whether or not conformation and the fulvalenediyl scaffold affect the formation of the Co–Co bonds, a *gauche* isomer of 2^+ (Figure S1 in the Supporting Information) was obtained as a minimum on the potential energy surface, which has a longer Co–Co bond length (2.986 Å) but is more unstable than the *anti* isomer by about 2.5 kcal mol^{−1} presumably as a result of steric crowding. The slight bending of SOMO and relatively longer Co–Co bond length in 1^+ are thus because of the constraint imposed by the fulvalenediyl scaffold.

The identity and bonding nature of radical cations were further investigated by EPR, IR, and UV/Vis spectroscopy. The EPR spectrum (Figure 3 a) of $1^+[\text{Al}(\text{OR}_{\text{Me}})_4]^-$ solution at 273 K displays a fifteen-line signal ($g = 2.0253$, $a = 9.97$ G) coupling with two equivalent cobalt atoms (^{59}Co , $I = 7/2$), which is confirmed by simulation (Figure 3 c). In the EPR spectrum of $2^+[\text{Al}(\text{OR}_{\text{H}})_4]^-$ (Figure 3 b), only thirteen of the expected fifteen lines are resolved ($g = 2.0295$, $a = 9.45$ G) and other two lines are unresolved. No better spectrum was obtained by changing temperatures of the samples during measurements. The C=O stretching frequencies shown in their solid IR spectra (Figures S3 and S4) increase from

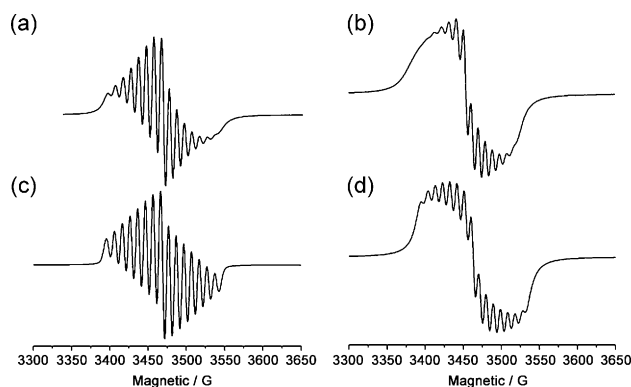


Figure 3. Experimental (top) and simulated (bottom) EPR spectra for 1^+ and 2^+ . a) EPR spectrum of 1×10^{-2} M solutions of $1^+[\text{Al}(\text{OR}_{\text{Me}})_4]^+$ in CH_2Cl_2 at 273 K. b) EPR spectrum of 1×10^{-2} M solutions of $2^+[\text{Al}(\text{OR}_{\text{H}})_4]^+$ in CH_2Cl_2 at 273 K.

neutral parent molecules to radical cations, consistent with the shortening of C–O bond lengths upon oxidation. The UV/Vis absorption spectra of $1^+[\text{Al}(\text{OR}_{\text{Me}})_4]^+$ and $2^+[\text{Al}(\text{OR}_{\text{H}})_4]^+$ solutions show two characteristic absorptions in the region of 520–750 nm (Figure 4). Judging from the time-

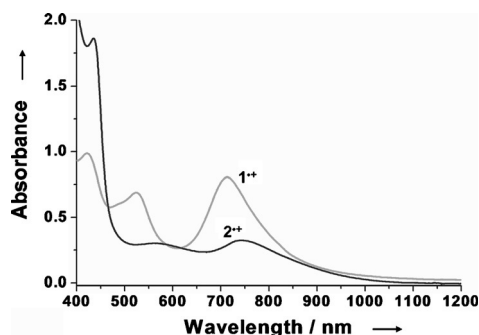
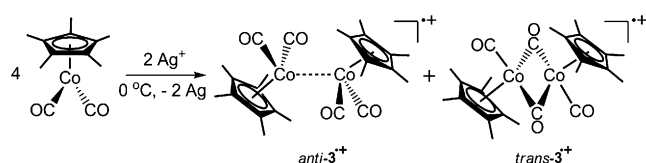


Figure 4. Absorption spectra of 1×10^{-4} M $1^+[\text{Al}(\text{OR}_{\text{Me}})_4]^+$ and $2^+[\text{Al}(\text{OR}_{\text{H}})_4]^+$ in CH_2Cl_2 at 273 K.

dependent DFT (TD-DFT) calculations at UB3LYP/6-311 + G(d,p)/LanL2DZ (Figure S6 and S7, Tables S3 and S4), these absorptions are mainly assigned to HOMO(β) \rightarrow LUMO(β) and HOMO-2(β) \rightarrow LUMO(β) electronic transitions. It is worth mentioning that these spin orbitals are rather delocalized over metal centers and ligands.

Further experimental work leads to an interesting isomerism of the Co–Co hemi-bond as a result of the replacement of Cp^* . The reaction of $\text{Cp}^*\text{Co}(\text{CO})_2$ with a half equiv of $\text{Ag}[\text{Al}(\text{OR}_{\text{F}})_4]$ ($\text{OR}_{\text{F}} = (\text{OC}(\text{CF}_3)_3)^{[11]}$) resulted in a brown solution of $3^+[\text{Al}(\text{OR}_{\text{F}})_4]^+$ (Scheme 2). Cooling the solution of $3^+[\text{Al}(\text{OR}_{\text{F}})_4]^+$ afforded reddish brown crystals, which



Scheme 2. Synthesis of isomeric cobalt radical cations of 3^+ .

were identified as two isomers (*anti*- 3^+ and *trans*- 3^+) with a 1:1 molar ratio by X-ray crystallographic analysis. Variable-temperature solution EPR spectra of $3^+[\text{Al}(\text{OR}_{\text{F}})_4]^+$ display broad signals lacking hyperfine splitting, indicating a rapid interchange of two isomers in the solution (Figure S2). The UV/Vis absorption spectrum of 3^+ (Figure S5 in the Supporting Information) is similar to those of 1^+ and 2^+ . Compared to those of 1^+ and 2^+ , the IR spectrum (Figure S3) of solid 3^+ shows an additional C=O stretching mode at lower frequency (1863 cm^{-1}), which is assigned to bridging CO groups. It is worth noting that only the radical with terminal carbonyls (i.e. *anti*- 3^+) was found in the previous solution studies.^[9a] Nonetheless, a similar equilibrium between *trans*- and *anti*-bimetallic radical cations of osmium was observed during the anode electrochemical oxidation of $\text{Os}_2\text{Cp}^*(\mu\text{-CO})_2(\text{CO})_2$, but this has not been structurally identified.^[15]

Single crystal X-ray diffraction shows that 3^+ is composed of two distinctly different isomers, *anti*- 3^+ and *trans*- 3^+ , which co-crystallize (Figure 5). The former has the *anti* conforma-

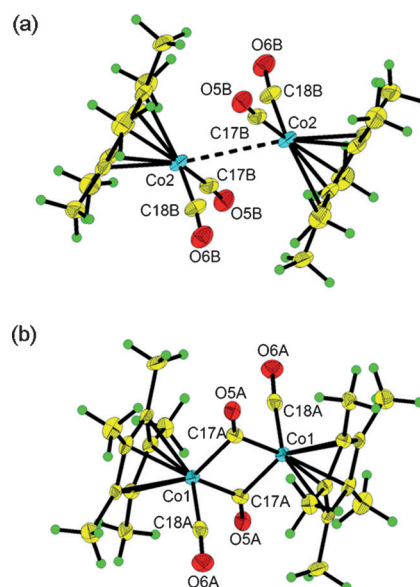


Figure 5. Thermal ellipsoid (50%) drawings of *anti*- 3^+ and *trans*- 3^+ . Yellow, carbon; green, hydrogen; red, oxygen; blue, cobalt. a) *anti*- 3^+ . Selected bond lengths [Å] and angles [deg]: Co2–Co2 3.074(2), Co2–C17B 1.783(5), Co2–C18B 1.783(5), C17B–O5B 1.133(6), C18B–O6B 1.128(6); C17B–Co2–C18B 101.0(2), Co2–C17B–O5B 173.7(5), Co2–C18B–O6B 174.3(5). b) *trans*- 3^+ . Selected bond lengths [Å] and angles [deg]: Co1–Co1 2.6208(16), Co1–C17A 1.951(5), Co1–C18A 1.813(5), C17A–O5A 1.158(6), C18A–O6A 1.133(6); C17A–Co1–C18A 95.5(2), Co1–C17A–O5A 138.1(4), Co1–C18A–O6A 176.5(4).

tion with a Co–Co bond unsupported by bridging carbonyl ligands, while the latter exhibits a *trans* configuration with two bridging CO groups. Similar to 1^+ and 2^+ , Co–C(O) bonds slightly lengthen while OC–Co–CO angles become wider in *anti*- 3^+ compared to neutral **3**. In *trans*- 3^+ , Co–C(O) and C–O bond lengths of bridging CO are longer than those of terminal CO. The Co–Co bond length in *anti*- 3^+ (3.074(2) Å) is slightly longer than that in 2^+ , while the Co–Co bond length (2.6208(16) Å) in *trans*- 3^+ is close to expected for a Co–Co single bond.^[13]

The observation of two distinct structures is verified by DFT calculations on single point energies at the (U)B97-D/6-311 + G(3df,2p)/LanL2DZ level. *Anti-3⁺* is more less stable than *trans-3⁺* but only by about 0.98 kcalmol⁻¹. In contrast, *anti-2⁺* is more stable than *trans-2⁺* by about 5.2 kcalmol⁻¹, which accounts for the experimental observation that *anti-3⁺* and *trans-3⁺* coexist in one crystal while only *anti-2⁺* is found in the solid state (i.e. *2⁺* in Figure 1b). The bonding in *anti-3⁺* resembles *anti-2⁺* (Figure S8) with slightly less bond order caused by the steric and electronic effects. Calculations indicate an absence of Co–Co bond in *trans-3⁺* (Figure S9) despite spin density is largely localized on two cobalt atoms.^[16]

We have described the isolation, characterization and crystal structures of a class of dicobalt metalloradicals (*1⁺*, *2⁺*, *anti-3⁺* and *trans-3⁺*). The formation of these dimer radicals proceeds possibly by a radical-substrate mechanism (*R⁺* + *R*). The long Co–Co bonds in *1⁺*, *2⁺*, and *anti-3⁺* may be rationalized by a simple three-electron bonding model as formed by the interaction of a mono-cobalt radical cation center with lone pair electrons of another cobalt atom, leading to a bond order of 1/2 or less, analogues to three-electron σ -bonds (Figure S10) of main group elements.^[10,17,18] To the best of our knowledge, *2⁺* and *anti-3⁺* are the first stable thus isolable examples that feature an unsupported metal–metal hemi-bond, and coexisting of *anti-3⁺* and *trans-3⁺* in one crystal is rare in the field of dinuclear metalloradical chemistry. The work suggests that more stable examples of metal–metal hemi-bonds may be accessible by using metal carbonyls together with large and weakly coordinating anions.

Keywords: cations · metalloradicals · metal–metal bonds · unsupported bonds · X-ray diffraction

How to cite: *Angew. Chem. Int. Ed.* **2015**, *54*, 9084–9087
Angew. Chem. **2015**, *127*, 9212–9215

- [1] F. A. Cotton, C. A. Murillo, R. A. Walton, *Multiple bonds between metal atoms*, 3rd ed., Springer, New York, NY, **2005**.
- [2] a) N. Wheatley, P. Kalck, *Chem. Rev.* **1999**, *99*, 3379; b) L. H. Gade, *Angew. Chem. Int. Ed.* **2000**, *39*, 2658; *Angew. Chem.* **2000**, *112*, 2768; c) I. Resa, E. Carmona, E. Gutierrez-Puebla, A. Monge, *Science* **2004**, *305*, 1136; d) H. Lei, J. Guo, J. C. Fetting, S. Nagase, P. P. Power, *J. Am. Chem. Soc.* **2010**, *132*, 17399; e) M. S. Hill, P. B. Hitchcock, R. Pongtavornpinyo, *Science* **2006**, *311*, 1904; f) S. Friedrich, H. Memmler, L. H. Gade, W.-S. Li, M. McPartlin, *Angew. Chem. Int. Ed. Engl.* **1994**, *33*, 676; *Angew. Chem.* **1994**, *106*, 705; g) R. S. Sternal, C. P. Brock, T. J. Marks, *J. Am. Chem. Soc.* **1985**, *107*, 8270; h) S. P. Green, C. Jones, A. Stasch, *Science* **2007**, *318*, 1754; i) C. F. Putnik, J. J. Welter, G. D. Stucky, M. J. D'Aniello, Jr., B. A. Sosinsky, J. F. Kirner, E. L. Muetterties, *J. Am. Chem. Soc.* **1978**, *100*, 4107; j) C. R. Hess, T. Weyhermüller, E. Bill, K. Wieghardt, *Angew. Chem. Int. Ed.* **2009**, *48*, 3703; *Angew. Chem.* **2009**, *121*, 3758; k) M. Herberhold, G. X. Jin, *Angew. Chem. Int. Ed. Engl.* **1994**, *33*, 964; *Angew. Chem.* **1994**, *106*, 1016; l) J. Chai, H. Zhu, A. C. Stückl, H. W. Roesky, J. Magull, A. Bencini, A. Caneschi, D. Gatteschi, *J. Am. Chem. Soc.* **2005**, *127*, 9201; m) P. L. Arnold, J. McMaster, S. T. Liddle, *Chem. Commun.* **2009**, 818.
- [3] a) M. L. Singleton, N. Bhuvanesh, J. H. Reibenspies, M. Y. Darensbourg, *Angew. Chem. Int. Ed.* **2008**, *47*, 9492; *Angew. Chem.* **2008**, *120*, 9634; b) T. Liu, M. Y. Darensbourg, *J. Am. Chem. Soc.* **2007**, *129*, 7008; c) J. M. Camara, T. B. Rauchfuss, *Nat. Chem.* **2012**, *4*, 26; d) A. Jablonskytė, J. A. Wright, S. A. Fairhurst, J. N. T. Peck, S. K. Ibrahim, V. S. Oganessian, C. J. Pickett, *J. Am. Chem. Soc.* **2011**, *133*, 18606.
- [4] M. G. Campbell, D. C. Powers, J. Raynaud, M. J. Graham, P. Xie, E. Lee, T. Ritter, *Nat. Chem.* **2011**, *3*, 949.
- [5] a) P. Aguirre-Etcheverry, D. O. Hare, *Chem. Rev.* **2010**, *110*, 4839; b) M. H. Chisholm, J. S. D'Acchioli, B. D. Pate, N. J. Patmore, N. S. Dalal, D. J. Zipse, *Inorg. Chem.* **2005**, *44*, 1061; c) F. A. Cotton, L. M. Daniels, C. A. Murillo, D. J. Timmons, C. C. Wilkinson, *J. Am. Chem. Soc.* **2002**, *124*, 9249; d) Y. Yan, J. T. Mague, J. P. Donahue, S. Sproules, *Chem. Commun.* **2015**, *51*, 5482.
- [6] E. F. van der Eide, P. Yang, E. D. Walter, T. Liu, R. M. Bullock, *Angew. Chem. Int. Ed.* **2012**, *51*, 8361; *Angew. Chem.* **2012**, *124*, 8486.
- [7] a) K. Gao, N. Yoshikai, *J. Am. Chem. Soc.* **2013**, *135*, 9279; b) B. Punji, W. Song, G. A. Shevchenko, L. Ackermann, *Chem. Eur. J.* **2013**, *19*, 10605; c) T. Zheng, H. Sun, Y. Chen, X. Li, S. Dürr, U. Radius, K. Harms, *Organometallics* **2009**, *28*, 5771.
- [8] K. C. Mondal, P. P. Samuel, H. W. Roesky, E. Carl, R. Herbst-Irmer, D. Stalke, B. Schwederski, W. Kaim, L. Ungur, L. F. Chibotaru, M. Hermann, G. Frenking, *J. Am. Chem. Soc.* **2014**, *136*, 1770.
- [9] a) A. Nafady, P. J. Costa, M. J. Calhorda, W. E. Geiger, *J. Am. Chem. Soc.* **2006**, *128*, 16587; b) A. Nafady, W. E. Geiger, *Organometallics* **2008**, *27*, 5624.
- [10] a) S. Zhang, X. Wang, Y. Sui, X. Wang, *J. Am. Chem. Soc.* **2014**, *136*, 14666; b) S. Zhang, X. Wang, Y. Su, Y. Qiu, Z. Zhang, X. Wang, *Nat. Commun.* **2014**, *5*, 4127.
- [11] I. Krossing, *Chem. Eur. J.* **2001**, *7*, 490.
- [12] X-ray data for *1⁺*, *2⁺* and *3⁺* are listed in the Table S1 in the Supporting Information. CCDC 1038780, 1038781, 1038782 contain the supplementary crystallographic data for this paper. These data can be obtained free of charge from The Cambridge Crystallographic Data Centre via www.ccdc.cam.ac.uk/data_request/cif.
- [13] L. Pauling, *Proc. Natl. Acad. Sci. USA* **1976**, *73*, 4290.
- [14] All calculations were performed using the Gaussian09 program suite. Gaussian09, Revision B.01, M. J. Frisch, G. W. Trucks, H. B. Schlegel, G. E. Scuseria, M. A. Robb, J. R. Cheeseman, G. Scalmani, V. Barone, B. Mennucci, G. A. Petersson, H. Nakatsuji, M. Caricato, X. Li, H. P. Hratchian, A. F. Izmaylov, J. Bloino, G. Zheng, J. L. Sonnenberg, M. Hada, M. Ehara, K. Toyota, R. Fukuda, J. Hasegawa, M. Ishida, T. Nakajima, Y. Honda, O. Kitao, H. Nakai, T. Vreven, Jr., J. A. Montgomery, J. E. Peralta, F. Ogliaro, M. Bearpark, J. J. Heyd, E. Brothers, K. N. Kudin, V. N. Staroverov, T. Kieth, R. Kobayashi, J. Normand, K. Raghavachari, A. Rendell, J. C. Burant, S. S. Iyengar, J. Tomasi, M. Cossi, N. Rega, N. J. Millam, M. Klene, J. E. Knox, J. B. Cross, V. Bakken, C. Adamo, J. Jaramillo, R. Gomperts, R. E. Stratmann, O. Yazyev, A. J. Austin, R. Cammi, C. Pomelli, J. W. Ochterski, R. L. Martin, K. Morokuma, V. G. Zakrzewski, G. A. Voth, P. Salvador, J. J. Dannenberg, S. Dapprich, A. D. Daniels, Ö. Farkas, J. B. Foresman, J. V. Ortiz, J. Cioslowski, D. J. Fox, Gaussian, Inc., Wallingford CT, **2010**.
- [15] D. R. Laws, R. M. Bullock, R. Lee, K. Huang, W. E. Geiger, *Organometallics* **2014**, *33*, 4716.
- [16] J. C. Green, M. L. H. Green, G. Parkin, *Chem. Commun.* **2012**, *48*, 11481.
- [17] L. Pauling, *J. Am. Chem. Soc.* **1931**, *53*, 3225.
- [18] K. Asmus, *Acc. Chem. Res.* **1979**, *12*, 436.

Received: April 14, 2015

Revised: May 9, 2015

Published online: June 12, 2015